

Piezoresponse through a ferroelectric nanotube wall

Stephen S. Nonnenmann, Eric M. Gallo, Michael T. Coster, Gregory R. Soja, Craig L. Johnson, Rahul S. Joseph, and Jonathan E. Spanier^{a)}
Department of Materials Science and Engineering, Drexel University, Philadelphia, Pennsylvania 19104, USA

(Received 14 July 2009; accepted 21 October 2009; published online 8 December 2009)

We report on the controlled local switching and imaging of local ferroelectric polarizations oriented perpendicular to the long axis of a lead zirconate titanate (PZT) nanotube. Piezoresponse force microscopy and ferroelectric piezoelectric hysteresis data indicate stable polarizations oriented along the radial, finite-thickness direction can be formed in a nanoshell geometry. The results of infrared spectroscopy and of the character of as-found polarizations are consistent with recent findings linking surface chemical environment to ferroelectric stability and to orientation of ferroelectric polarizations. © 2009 American Institute of Physics. [doi:10.1063/1.3263714]

Nanoscale ferroelectrics (FEs) exhibit size-dependent phenomena^{1–10} not observed in bulk, generating interest in their physics and applications. Among recent studies are theoretical and proximal probe experimental investigations in which unusual dipole ordering,^{1,2} size- and/or shape-driven FE phase transitions and transition temperatures,^{3,8} and enhanced axial polarizations^{3,4} were reported. The stabilizing effect of molecular adsorbates⁸ and of surface-induced strains⁵ in reinforcing out-of-plane polarizations against depolarizing fields has been observed in films and in high aspect ratio, large surface-to-volume nanostructures alike.^{6–9}

Template-assisted fabrication techniques using materials such as anodic aluminum oxide (AAO) have expanded synthetic options for experimental realization of low-dimensional FE in arrays of nanotubes,^{11,12} nanowires,^{8,13} nanoislands,¹⁴ and nanodots,¹⁵ thereby permitting study of finite-size and shape effects, significant for application in higher-density nonvolatile memories. Investigations of size effects in FE thin films have employed piezoresponse force microscopy (PFM) to observe the local FE response as induced via a conductive tip. Reports of PFM of one-dimensional-like nanostructures such as nanowires^{8,13,16,17} and nanotubes^{11,12} are scarce; in nanotubes, only FE hysteresis across the entire tube diameter has been measured, leaving limited knowledge of the domain morphology and of the FE response within the nanoshell. Here, we report on the use of Au–Pb(Zr_{0.52}Ti_{0.48})O₃ (PZT) coaxial cylindrical nanowires to investigate the stability and switching of FE domains oriented along the finite, shell-normal direction.

Coaxial nanowires were prepared using template-assisted growth, sol-gel processing,^{11,12} and electrochemical deposition techniques.¹⁸ AAO templates were produced from high purity Al sheets (Alfa Aesar Puratronic 99.9995% #43777) via a two-step anodization process in oxalic acid (0.3M, 1 °C, 30 V). Templates were immersed in a PZT alkoxide precursor (Chemat 9103), air dried and then calcined, first for 1 h at 300 °C to remove organics, and then 5 h at 700 °C to produce the perovskite nanoshells. The templates were each backcoated with a thermally evaporated Ag layer and a passivating layer (Sally Hansen Hard as Nails™), allowing cathodic reduction of an Au plating bath

(Technic 25, $J=1$ mA/cm², 1 h) to form Au-PZT coaxial nanowires, and then dissolved in 6M NaOH (VWR 3246) to create freestanding nanowires. Electron-beam lithographically defined windows in e-beam resist were used to facilitate selective wet etching¹⁹ of the perovskite shell. The resist surface and etched patterns were coated with thermally evaporated Cr (10 nm) and Au (150 nm) and then placed in acetone (VWR 9002) to remove the resist, yielding electrically addressable nanowire core electrodes. Nanowire diameters and thicknesses were obtained by atomic force microscopy (Asylum Research MFP-3D) and transmission electron microscopy (TEM) (JEOL 2100), respectively. TEM [Fig. 1(a); selected area electron diffraction (inset)] and scanning electron microscopy (SEM) [Fig. 1(b)] images confirm structures are ≈ 5 μ m long, 50 nm in diameter, and 7 nm in shell thickness, with an average grain size of ≈ 5 nm. Shown in Fig. 1(b) is a SEM image (*false color*) of an electrically contacted coaxial nanowire, prior to proximal probe charac-

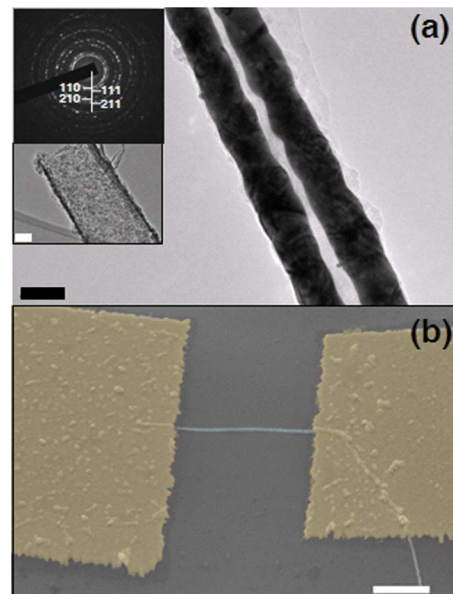


FIG. 1. (Color online) (a) TEM image of two 50 nm diameter Au-PZT core-shell nanowires, scalebar=50 nm. Upper inset, electron diffraction of a bundle of Au-PZT nanowires indexed as 110, 111, 210, and 211 of the perovskite form. Lower inset, empty 200 nm PZT nanotube, scalebar =50 nm. (b) SEM image of a single nanowire, scalebar=1 μ m.

^{a)}Electronic mail: spanier@drexel.edu.

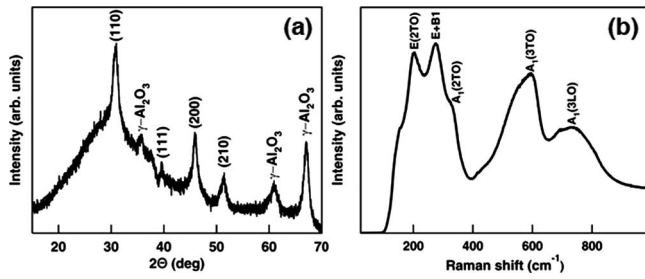


FIG. 2. (a), XRD of nanotubes within the AAO template. Indexed peaks are of tetragonal perovskite; all remaining indices are assigned to the AAO. (b) Raman spectrum of an individual 100 nm PZT nanotube in which the observed modes of tetragonal perovskite are denoted.

terization. Structures ranging from 50–240 nm in diameter, 3–10 μm long, and 7–30 nm in shell thickness (ζ) were prepared in this manner.

Structural characterizations of the coaxial nanowires were performed using x-ray diffraction (XRD) and Raman scattering spectroscopy. Plotted in Fig. 2(a) is the XRD collected from PZT nanotubes embedded within the AAO, possessing reflections from tetragonal perovskite PZT grown via sol-gel;²⁰ the other observed peaks are from the AAO template.²¹ It should be noted that the perovskite phase is present despite its small grain size (≈ 5 nm). This does not preclude the existence of a surface pyrochlore phase, previously shown as a 10% perovskite/pyrochlore phase ratio in identically prepared sol-gel PZT nanotubes with nanocrystalline grains.²² A representative Raman spectrum [Fig. 2(b)] (Renishaw 1000, 514.5-nm excitation) collected from an individual PZT nanoshell contains peaks near 205, 275, 325, 594, and 737 cm^{-1} ; these energies correspond to the irreps (phonon modes) E(2TO), E+B₁, A₁(2TO), A₁(3TO), and A₁(3LO) of perovskite PZT of the specified composition,¹³ respectively.

Proximal probe measurements were collected by scanning the topography of the nanowire [Fig. 3(a)], after which the tip was repositioned onto the nanowire surface and held in constant deflection feedback, where a slowly varying bias was applied to the nanowire core (± 18 V_{pp}, 0.05 Hz) while an ac bias was simultaneously applied (3 V_{pp}, 4 kHz) to the cantilever tip [Fig. 3(b)], thus enabling the collection of FE

hysteresis loops [Fig. 3(c)]. The coercive field E_C exhibits a $\approx \zeta^{-1}$ scaling. The observed positive vertical offsets, commonly attributed in thin films to the imprint behavior of a nonswitchable dead layer,²³ result from surface tension-induced strain gradients in the nanoshells, similar to the effects in graded ferroics.²⁴ Larger radius nanoshells hysteresis exhibited a negligible shift, while those of more extreme curvature displayed large offsets.

The local FE response across the smallest (radial) dimension of PZT nanoshells was collected by PFM (Asylum Research MFP-3D). Images were obtained using a Ti–Pt coated tip (Olympus Electrilever, $k \approx 2$ N/m, tip radius ≈ 15 nm) biased at 2 V while driven at 280 kHz, away from the cantilever resonance (77 kHz), as to minimize topographic contributions. During PFM imaging, the Au nanowire core was held at ground. The height map of a representative 100 nm diameter nanowire is shown in Fig. 3(a). The nanowire diameter appears larger due to tip-nanowire convolution effect, similar to other PFM studies of FE nanowires.^{16,17} Successive PFM phase contrast maps (range $+150^\circ$ to -50°) of the nanoshell polarization as-found [Fig. 3(d)], and following application of -10 V [Fig. 3(e)] and $+10$ V [Fig. 3(f)] while the tip was scanned over a region denoted by the dashed circles indicate an outward shell-normal polarization component in this region initially, with demonstrable reversible switching, respectively. Switching events were produced in deflection feedback point mode for a duration of 10–12 s. Following a writing event, the local phase signal associated with each written and switched domain was observed to be stable for the timescale investigated. No detectable change in contrast could be discerned among five successive scans following a writing event (70 min). A study of the long-term stability of written and switched domains, however, merits further study.

The image data in Figs. 3(d)–3(f) raise interesting questions regarding the origin and stability of polarizations oriented along the finite-thickness dimension in ultrathin films and nanostructures. Remarkably, an outward shell-normal (as opposed to in-plane) polarization is seen over some portions of the nanoshells in their as-found state, consistent with the orientation observed within ultrathin FEs possessing chemisorbed M (M=transition metal)–OH.⁶ The effective screening length of such adsorbates can be even shorter than those for metallic electrodes,⁹ thus mitigating the effect of the depolarizing fields that typically suppress the response in ultrathin films situated between two electrodes.¹⁰ Fourier transform infrared (FTIR) absorption spectra (Fig. 4) were collected (Varian Excalibur FTS-3000) using a diamond single reflection attenuated total reflectance prism. Nanowire suspensions were dried (150 $^\circ\text{C}$) and exchanged repeatedly in chloroform (BDH1109) to ensure the absence of free hydroxyl species. The suspension was evaporated onto the prism surface before accumulating spectra (128 scans, 2 cm^{-1} resolution). The estimated peak at ≈ 3650 cm^{-1} is assigned to M–OH (M=Zr,Ti) stretching modes,²⁵ indicative of surface-terminated chemisorbed hydroxyl species along the FE nanoshell. We note that no discernable stretching modes for either Pb–O or surface O–H were observed, consistent with their reduced thermodynamic stability.⁶ These adsorbates have been predicted to produce upwards and downwards polarization states, respectively. The large feature estimated at ≈ 2925 cm^{-1} results from C–H stretch-

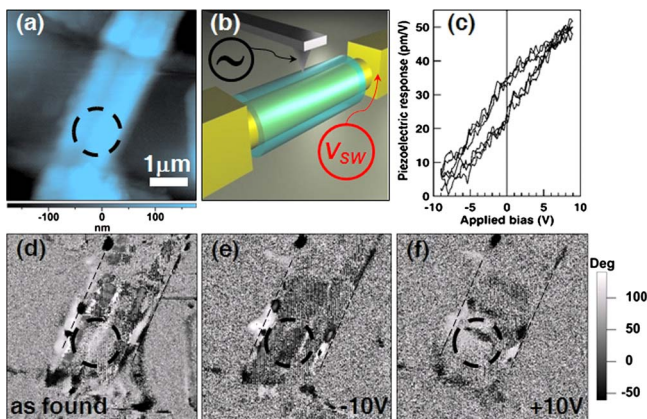


FIG. 3. (Color online) (a) Height map of a 100 nm Au-PZT coaxial nanowire. (b) Experimental scheme for collecting (c) FE piezoelectric hysteresis and (d)–(f) plane-normal piezoresponse phase contrast maps. (d) represents the “as-found” state with (e) and (f) revealing written negative and positive FE domains, respectively (dashed circles).

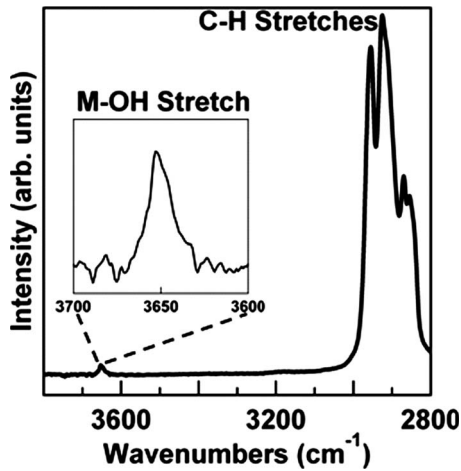


FIG. 4. FTIR spectrum of 100 nm PZT nanotubes. Inset shows an enlarged view of the 3650 cm^{-1} peak, resulting from surface terminated hydroxyl species. The large peak at 2925 cm^{-1} corresponds to C-H stretching modes.

ing modes of residual organics from the dried nanowire suspension.

We note that the absorbed species can play a role in the observed component of outward normal polarization and the vertical offset in the observed hysteresis in the as-found shell. The precise mechanism(s) influencing the domain stability after switching events [Figs. 3(e) and 3(f)], however, are not clear. The multitude of domain states observed throughout the length of the nanowire result from competing elastic and depolarizing effects within polycrystalline grains²⁶ [Fig. 1(a) inset], creating mixed 90° (gray or no contrast) and 180° (white/black contrast) domains. The values of ΔG (the reaction energy per adsorbate) for species relevant to the present experiments are in the range of $-0.2 < \Delta G < 1.95$ eV at 300 K.⁶ While several possible adsorbate and adatom species and/or oxygen vacancies may participate in screening, we propose that the locally intense electric field under the tip, produced by the application of the switching voltage (± 3 V_{pp}), is sufficiently large for these and other adsorbates to overcome the energetic barriers necessary for desorption and migration, and also for migration of vacancies toward or away from the surface of the written domain. Attempts to image the lateral piezoresponse (along the fast scan direction; minimal loading force) damaged the PZT nanoshell surface, making a full domain map of the nanoshell infeasible. The switching observed in Figs. 3(e) and 3(f), however, unambiguously show a shell-normal (or out-of-plane) component of polarization.

In conclusion, we have measured the FE response across the finite, radial dimension of template-fabricated Au-PZT cylindrical nanowires via PFM. Stable, switchable shell-normal oriented polar components are observed, as demonstrated by hysteresis and imaging of a switched domain state. The outward shell-normal components in the as-found nanoshell can be explained by the presence of M-OH

adsorbates, consistent with previous work of domain stability in thin films⁶ and nanowires.⁸ We believe these principles and methods will stimulate interest and develop new applications in low-dimensional systems of ferroelectrics and multiferroics.

We thank Zhorro Nikolov for assisting with FTIR, Terrence McGuckin for the sample interface, and Craig Johnson for performing TEM. We acknowledge the Materials Characterization Facility at Drexel for access to the TEM, XRD, and FTIR. This work was supported by the Army Research Office (Grant No. W911NF-08-1-0067). S.S.N and E.G. were also supported in part by the NSF-IGERT (Grant No. DGE-0221664), by the NSF GK-12 (Grant No. DGE-0538476), and by a NSF GRF (E.G.).

- ¹I. I. Naumov, L. Bellaiche, and H. Fu, *Nature (London)* **432**, 737 (2004).
- ²B. J. Rodriguez, X. S. Gao, L. F. Liu, W. Lee, I. I. Naumov, A. M. Bratkovsky, D. Hesse, and M. Alexe, *Nano Lett.* **9**, 1127 (2009).
- ³A. N. Morozovska, E. A. Eliseev, and M. D. Glinchuk, *Phys. Rev. B* **73**, 214106 (2006).
- ⁴D. Yadlovker and S. Berger, *Phys. Rev. B* **71**, 184112 (2005).
- ⁵Z. H. Zhou, X. S. Gao, J. Wang, K. Fujihara, S. Ramakrishna, and V. Nagarajan, *Appl. Phys. Lett.* **90**, 052902 (2007).
- ⁶D. D. Fong, A. M. Kolpak, J. A. Eastman, S. K. Streiffer, P. H. Fuoss, G. B. Stephenson, C. Thompson, D. M. Kim, K. J. Choi, and C. B. Eom, *Phys. Rev. Lett.* **96**, 127601 (2006).
- ⁷V. Garcia, S. Fusil, K. Bouzehouane, S. Enouz-Vedrenne, N. D. Mathur, A. Barthelemy, and M. Bibes, *Nature (London)* **460**, 81 (2009).
- ⁸J. Spanier, A. Kolpak, J. Urban, I. Grinberg, L. Ouyang, W. Yun, A. Rappe, and H. Park, *Nano Lett.* **6**, 735 (2006).
- ⁹N. Sai, A. M. Kolpak, and A. M. Rappe, *Phys. Rev. B* **72**, 020101 (2005).
- ¹⁰J. Junquera and P. Ghosez, *Nature (London)* **422**, 506 (2003).
- ¹¹B. A. Hernandez, K.-S. Chang, E. R. Fisher, and P. K. Dorhout, *Chem. Mater.* **14**, 480 (2002).
- ¹²Y. Luo, I. Szafraniak, N. D. Zakharov, V. Nagarajan, M. Steinhart, R. B. Wehrspohn, J. H. Wendorff, R. Ramesh, and M. Alexe, *Appl. Phys. Lett.* **83**, 440 (2003).
- ¹³X. Y. Zhang, X. Zhao, C. W. Lai, J. Wang, and J. Y. Dai, *Appl. Phys. Lett.* **85**, 4190 (2004).
- ¹⁴W. Lee, H. Han, A. Lotnyk, M. A. Schubert, S. Senz, M. Alexe, D. Hesse, S. Baik, and U. Goesele, *Nat. Nanotechnol.* **3**, 402 (2008).
- ¹⁵S. O'Brien, L. Brus, and C. B. Murray, *J. Am. Chem. Soc.* **123**, 12085 (2001).
- ¹⁶J. Wang, C. S. Sandu, E. Colla, Y. Wang, W. Ma, R. Gysel, H. J. Trodahl, N. Setter, and M. Kuball, *Appl. Phys. Lett.* **90**, 133107 (2007).
- ¹⁷Z. Wang, J. Hu, and M.-F. Yu, *Appl. Phys. Lett.* **89**, 263119 (2006).
- ¹⁸M. Liu, X. Li, H. Imrane, Y. Chen, T. Goodrich, Z. Cai, K. S. Ziemer, J. Y. Huang, and N. X. Sun, *Appl. Phys. Lett.* **90**, 152501 (2007).
- ¹⁹S. Ezhilvalavan and V. D. Samper, *Appl. Phys. Lett.* **86**, 072901 (2005).
- ²⁰Z. Chen, C. Yang, B. Li, M. Sun, and B. Yang, *J. Cryst. Growth* **285**, 627 (2005).
- ²¹S. G. Yang, T. Li, L. S. Huang, T. Tang, J. R. Zhang, B. X. Gu, Y. W. Du, S. Z. Shi, and Y. N. Lu, *Phys. Lett. A* **318**, 440 (2003).
- ²²J. Kim, S. A. Yang, Y. C. Choi, J. K. Han, K. O. Jeong, Y. J. Yun, D. J. Kim, S. M. Yang, D. Yoon, and H. Cheong, *Nano Lett.* **8**, 1813 (2008).
- ²³M. Alexe, C. Harnagea, D. Hesse, and U. Goesele, *Appl. Phys. Lett.* **79**, 242 (2001).
- ²⁴Z. Ban, S. P. Alpay, and J. V. Mantese, *Phys. Rev. B* **67**, 184104 (2003).
- ²⁵Z. Weishauptová, V. Machovic, M. Novotná, and J. Medek, *Mater. Chem. Phys.* **102**, 219 (2007).
- ²⁶J. Wang and M. Kamlah, *Appl. Phys. Lett.* **93**, 042906 (2008).